Multiphase Hydrodynamics and Distribution Characteristics in a Monolith Bed Measured by Optical Fiber Probe

Yuan Zhou
State Key Laboratory of Chemical Resource Engineering, School of Chemical Engineering, Beijing University of Chemical Technology, Beijing 100029, China

State Key Laboratory of Multiphase Complex Systems, Institute of Process Engineering, Chinese Academy of Sciences, Beijing 100190, China

Milorad P. Dudukovic
Chemical Reaction Engineering Laboratory (CREL), Department of Energy, Environmental, and Chemical Engineering (EECE), Washington University in St. Louis, St. Louis, MO 6330

Muthanna H. Al-Dahhan
Department of Chemical and Biological Engineering, Missouri University of Science and Technology, Rolla, MO 65409

Hui Liu
State Key Laboratory of Chemical Resource Engineering, School of Chemical Engineering, Beijing University of Chemical Technology, Beijing 100029, China

DOI 10.1002/aic.14269
Published online October 30, 2013 in Wiley Online Library (wileyonlinelibrary.com)

The optical fiber probe has been for the first time applied to investigate the hydrodynamics and gas-phase distribution at high gas/liquid ratios in a two-phase flow monolith bed with 0.048 m diameter and 400 cpsi. Local hydrodynamic parameters including gas holdup, bubble frequency, bubble velocity, and bubble length in single channels were measured by 16 inserted single-point optical fiber probes within the bed under a nozzle as the liquid distributor. The following findings are reported. (1) The optical fiber probe can be used as an efficient and convenient technique for measuring local hydrodynamic parameters inside the channels of a monolith bed; (2) within the range of high gas/liquid ratios under which experiments were conducted, churn flow regime occurred. In this regime, the monolith bed radial distribution of gas holdup, bubble frequency, bubble velocity, and bubble length is nonuniform in nature. © 2013 American Institute of Chemical Engineers *AIChE J*, 60: 740–748, 2014
Keywords: monolith reactor, optical fiber probe, hydrodynamics, scale-up effect

Introduction

A monolith bed consists of a bundle of separated parallel channels with channel sizes of 1–3 mm, where the channel wall is coated with catalytic or active materials to form a functional layer of 20–150 μm. For multiphase applications, gas and liquid flow through the channels upward or downward cocurrently or countercurrently, and the reactants are transformed in the presence of the functional layer. It has been reported that monolith beds or multiphase monolith reactors (MMRs) are promising for many catalytic gas-liquid-solid reactions encountered in chemical, petrochemical, biochemical, and environmental processes.[1–3] It is demonstrated that MMRs offer advantages including low pressure drop, high geometric surface area, good mass transfer, and mechanical integrity,[4–6] compared with the traditional multiphase reactors such as trickle beds and slurry bubble columns. However, potential nonuniform fluid distribution and, thus, lower reactor effectiveness; difficulty and higher cost in extruding and installation of large industrial scale and heat-transfer limitation are the disadvantages of monolith reactors. For these reactors, understanding the fluid distribution and gas-liquid hydrodynamics in the channels is an important issue because it is closely related to the mass-transfer[7–9] and reaction performances[10] of the processes.

Gas-liquid flows have been investigated in a single channel or capillary scale mainly in the Taylor flow regime.[7,10–14] In general, the gas-liquid flow in a single capillary may be to some extent analogous to the flow in a monolith bed scale as a whole. However, it has been reported that in a monolith bed, nonuniform distribution of gas and liquid at the entrance of the bed is frequently encountered.[15–23] The nonuniformity of phase distribution across a monolith bed is largely dependent on the type of liquid and gas distributor and superficial velocities of gas and liquid.[16,24,25] These previous studies were mainly focused on the measurements of liquid

Correspondence concerning this article should be addressed to M. H. Al-Dahhan at aldahhanm@mst.edu.

distribution in monolith beds, but seldom measuring the hydrodynamic parameters typical of the Taylor flow due to the limitation of the measuring techniques. However, for the industrial application of monolith reactors, we need to scale-up gas-liquid flows from a single capillary to a monolith bed. Therefore, the hydrodynamics needs to be further investigated within the monolith bed structure. Furthermore, some of the key hydrodynamic parameters such as liquid- and gas-phase velocities and holdups inside the channels of a monolithic bed have not yet been known and quantified. These are needed for integrating kinetics and hydrodynamics for reactor scale performance modeling when the flow is not uniformly distributed and for validation of computational fluid dynamics (CFD). Conversely, there was favoritism of the Taylor flow in the literature due to the superior mass transfer in this flow regime,[7,9] which is essential for a variety of mass-transfer limiting reaction processes. However, Taylor flow occurs at high liquid linear velocity and low gas/liquid ratio, which are not typical of most practical processes[26] such as selective hydrogenation, but rather a high gas/liquid ratio is more favored to achieve high conversions and to lower the rate of catalyst deactivation. Hence, there is need to extend the investigation of the two-phase hydrodynamics to regimes other than Taylor flow.

The available techniques for measuring the two-phase hydrodynamics in an opaque monolith bed are lacking. The noninvasive techniques including liquid bottom collection,[18] gamma-ray computed tomography,[15,16,27,28] capacitance tomography,[22] and so forth, were confined to measure the phase hold-ups distribution. However, they are not suitable for characterizing bubble dynamics in individual channels of the bed, particularly bubbles and liquid slugs velocities. The use of nuclear magnetic resonance imaging for "visualizing," the dynamics of the two-phase flow in individual monolith channels[20,29] and hence evaluating hydrodynamic parameters like bubble velocity and length, is a very time consumption in data processing and is limited to a small scale of beds.

Therefore, the major objective of the present work is to experimentally investigate the hydrodynamics and the distributions of local gas holdup, bubble frequency, bubble velocity, and bubble length in a gas-liquid monolith bed at high gas/liquid ratios. To this end, an optical fiber microprobe, which has been successfully utilized in bubble column and slurry bubble column,[30–32] has been implemented for the first time to measure the above mentioned hydrodynamic parameters at different radial and axial locations across the section of a monolith bed. Furthermore, comparisons were made to show the differences in hydrodynamics values between those obtained within the central channel and the averaged values over the bed as a whole to assess the extent of the uniformity or the nonuniformity in the bed.

Experimental Methods

Monolith reactor flow system

The experimental setup, as shown in Figure 1, consists of a monolith section, distributor, and liquid and gas delivery systems. The monolith is made of cordierite, with a diameter of 1.9 in (0.048 m), a length of 6.0 in (0.152 m), and cell density of 400 cells per square inch (cpsi). The flow channels are of square cross section with a dimension of nominally 1 mm along each side. The monolith was fixed inside a cold flow model Plexiglas column of 0.051 m in diameter by

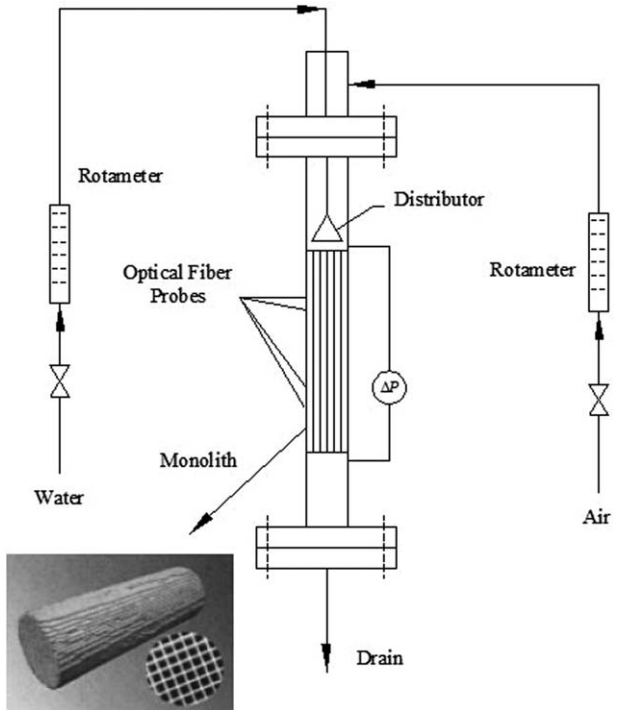

Figure 1. Monolith structure and experimental setup.

two Teflon gaskets, one at the top and the other at the bottom of the monolith bed. The gaskets were held in position by support rings at the top and bottom to seal the small gap between the column wall and the monolith and to prevent by-pass flow of gas or liquid near the column wall. In all experiments, a nozzle distributor as used by Roy and Al-Dahhan[15,24] was used to distribute the liquid. The cold model set up was operated in the cocurrent down-flow and continuous mode, using air as the gas phase and water as the liquid phase which is introduced at the top through a nozzle distributor (6 mm orifice diameter). Water and air together entered the monolith bed at the top and upon exiting were discharged to a drain. Water first introduced into the bed to well wet the monolith walls, then measurements were made after the two-phase flow reached steady state as reflected by steady and stable signals of gas holdup. In each experiment, three measurements were repeated and the reproducibility was found to be within 10%.

The flow conditions were specified at low liquid velocity ($\sim$0.075–0.1 m/s) and high gas/liquid ratio ($\sim$8–22), which are typical of the conditions of interest for existing commercial reactor applications[26] such as hydrogenation reactions of styrene, 1-octene and toluene.

Optical fiber probe and measurement procedure

For measuring bubble flow parameters in bubble column and slurry bubble column, a four-point optical probe technique was successfully adopted and implemented by Xue et al.[30,31] and Wu et al.[32] In this work, we transform this four-point optical probe into a single-point microprobe such that it could be used for the first time to measure hydrodynamic parameters in individual channels of a monolith bed. The optical fiber probe (Figure 2a) was made of the optical fiber (Figure 2b) 600 μm in diameter containing a glass core (200 μm), a cladding, and a protective layer. Because of the

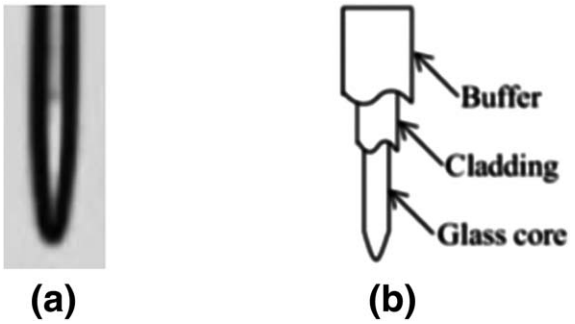

Figure 2. Optical fiber probe.

(a) a picture of the optical fiber probe and (b) schematic of the optical fiber.

small monolith channels of width 1 mm, only the glass core of 200 μm is inserted inside a particular channel in a careful machining. This is to ensure that the tip of the probe does not obstacle the flow of gas and liquid and does not affect the measurement.

A total of 16 optical fiber probes were inserted into selected channels at four different axial positions and four radial positions of the used monolithic bed. Due to the axial symmetry configuration of both the liquid distributor and the monolith bed, the liquid saturation distributions in the bed should exhibit radial symmetry, as reported by Roy and Al-Dahhan[15] and Al-Dahhan et al.[28] Consequently these probes were arranged as shown in Figure 3. In the figure, every point indicating a probe was named [Tip XY], in which X means the selected channel number at different radial positions and Y represents the axial distance from the top of the monolith bed. Here, $X = 1$, 2, 3, and 4 correspond to the radial positions in the monolith of $r/R = 0$, 0.25, 0.5, and 0.75, respectively; and $Y = 1$, 2, 3, and 4 refer to different axial distances from the top of the monolith bed of $H = 40$, 50, 102, and 112 mm, respectively. For example, Tip 12 is the second tip (axially) in the central channel (channel #1), as the tip is located at $r/R = 0$ and $H = 50$ mm.

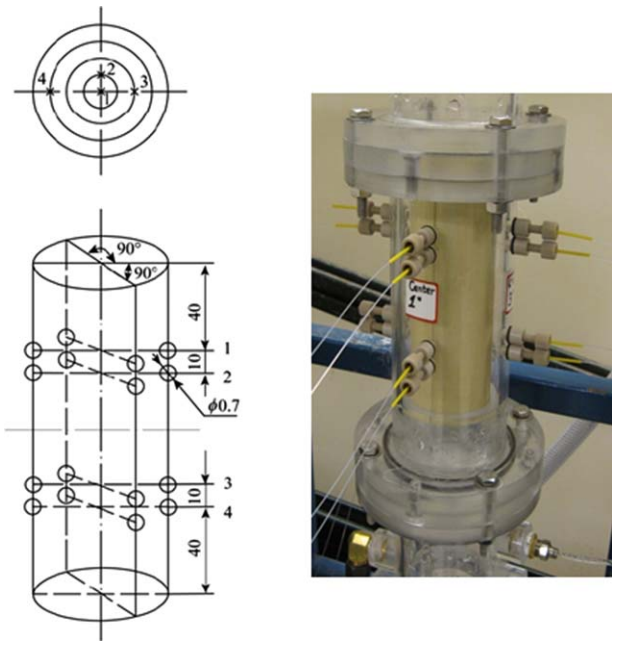

Figure 3. Configuration of optical fiber probes in the monolith bed (unit: mm).

[Color figure can be viewed in the online issue, which is available at wileyonlinelibrary.com.]

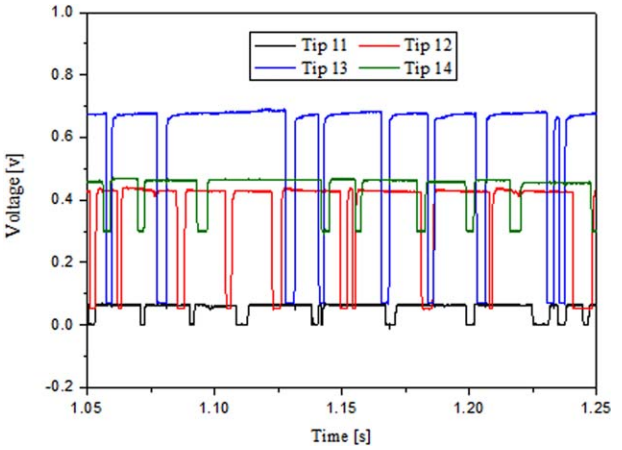

Figure 4. Responses of bubbles passing by the optical fiber probes fixed on four different axial positions in the central channel ($U_L = 0.1$ m/s, $U_G = 0.626$ m/s; Nozzle).

[Color figure can be viewed in the online issue, which is available at wileyonlinelibrary.com.]

All the probes were connected to an A/D unit and then a computer was used to record the output signals from probe at a sampling frequency of 40 kHz. In principle, when the optical fiber tip is in the liquid phase, the light is transferred into the liquid, establishing a baseline signal. When a bubble hits the fiber, the light reflects, and the voltage rise is captured by the electronic unit, leading to a peak. Typical signals of optical fiber probes are shown in Figure 4. It is evident that when gas bubble and liquid slug pass around the microprobe tip, the existence of gas and liquid phases can be clearly identified by the probe. However, the resolution of the probe is limited. For the present 1 mm channels, the probes mounted inside them will yield vague signals which are difficult to interpret if bubbles have a smaller size than that of the channels. Conversely, five distinct flow regimes might be observed for gas-liquid flows through a capillary,[11]

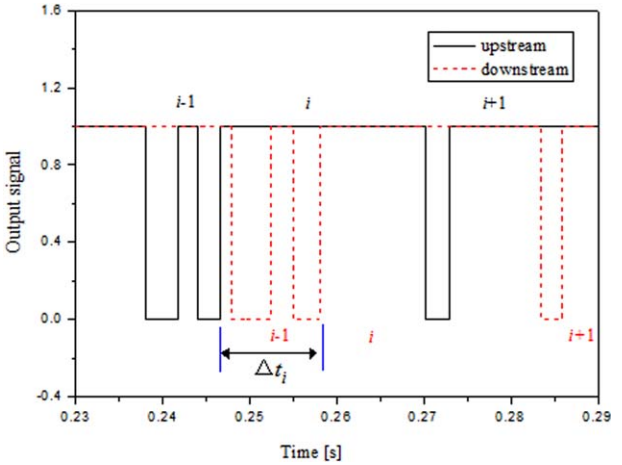

Figure 5. Bubble velocity obtained by optical fiber probes.

[Color figure can be viewed in the online issue, which is available at wileyonlinelibrary.com.]

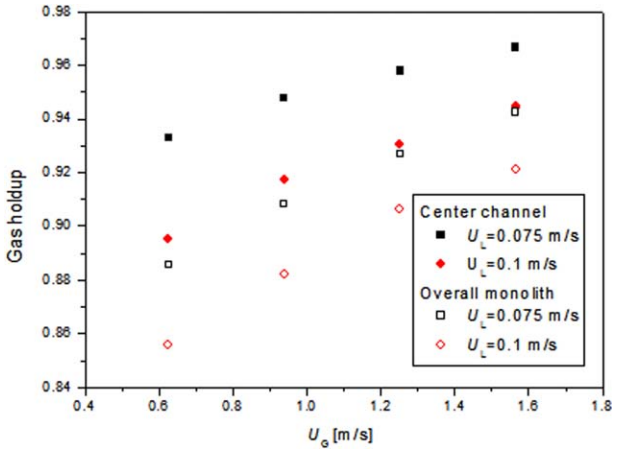

Figure 6. Gas holdup of both center channel and overall monolith with varying gas and liquid superficial velocities.

[Color figure can be viewed in the online issue, which is available at wileyonlinelibrary.com.]

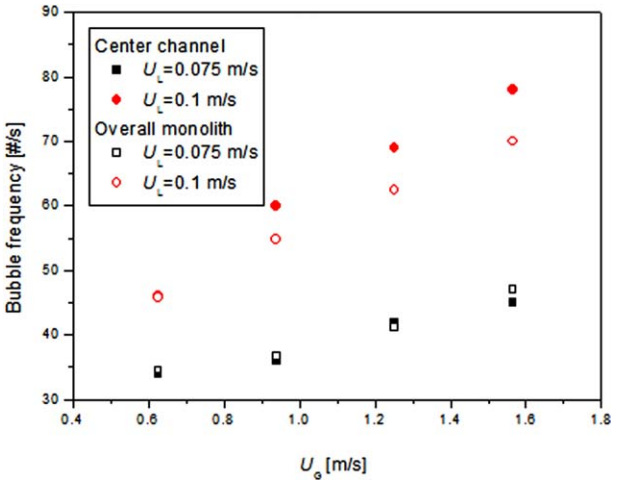

Figure 8. Bubble frequency of both center channel and overall monolith with the change of gas and liquid superficial velocities.

[Color figure can be viewed in the online issue, which is available at wileyonlinelibrary.com.]

that is, bubbly, slug bubbly, Taylor, churn turbulent and annulus flows, depending on the gas and liquid velocities. In this work, high gas/liquid ratios around 8–22 were used. Over the range of these operating conditions, the detected flow regime in the selected channels was found to be churn turbulent flow regime, in which very long gas bubbles and relatively short liquid slugs dominate in the channel. This is

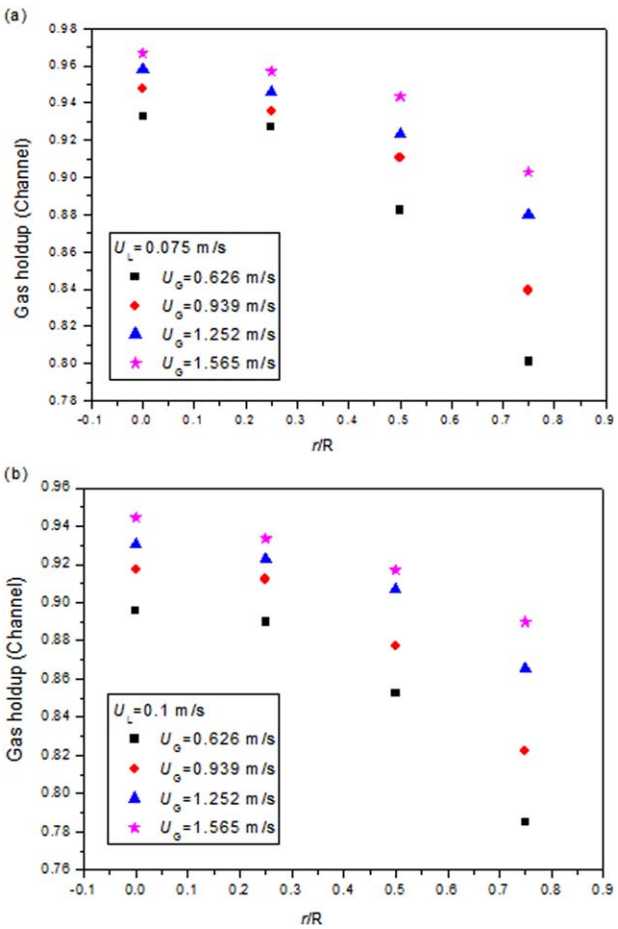

Figure 7. Radial distribution of gas holdup. (a) U_L = 0.075 m/s and (b) U_L = 0.1 m/s.

[Color figure can be viewed in the online issue, which is available at wileyonlinelibrary.com.]

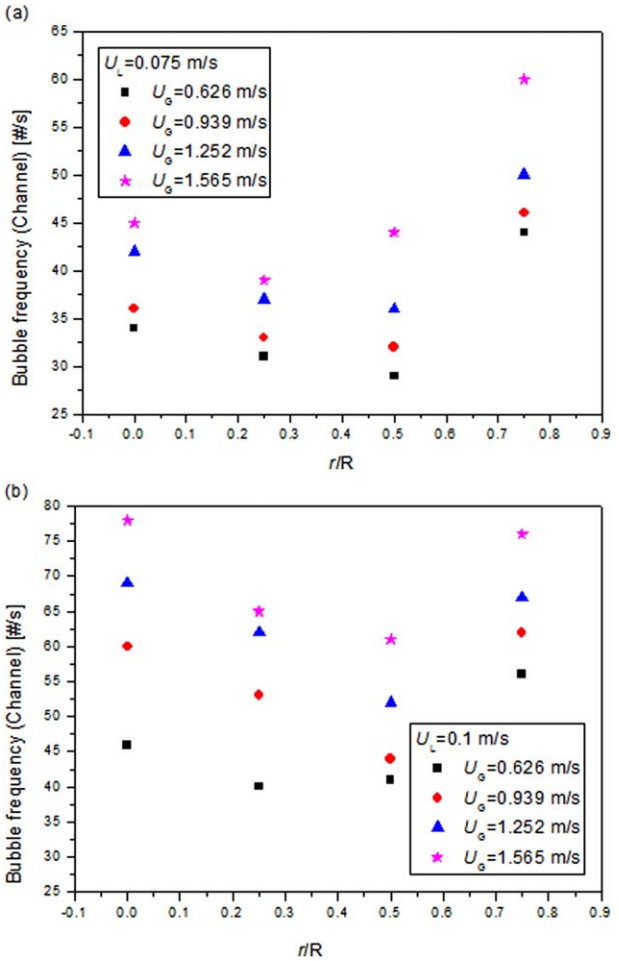

Figure 9. Radial distribution of bubble frequency. (a) U_L = 0.075 m/s and (b) U_L = 0.1 m/s.

[Color figure can be viewed in the online issue, which is available at wileyonlinelibrary.com.]

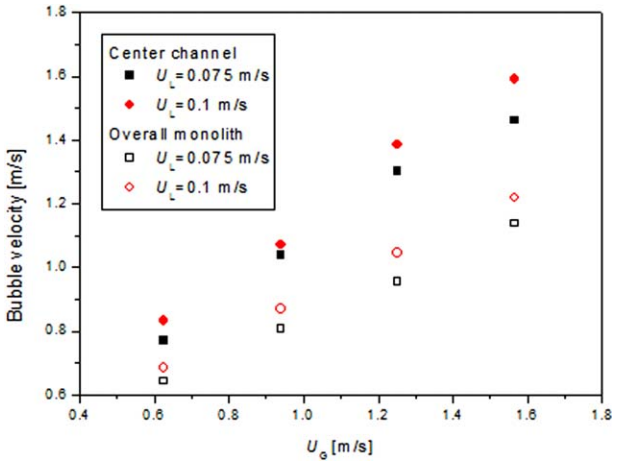

Figure 10. Bubble velocity of both center channel and overall monolith with varying gas and liquid superficial velocities.

[Color figure can be viewed in the online issue, which is available at wileyonlinelibrary.com.]

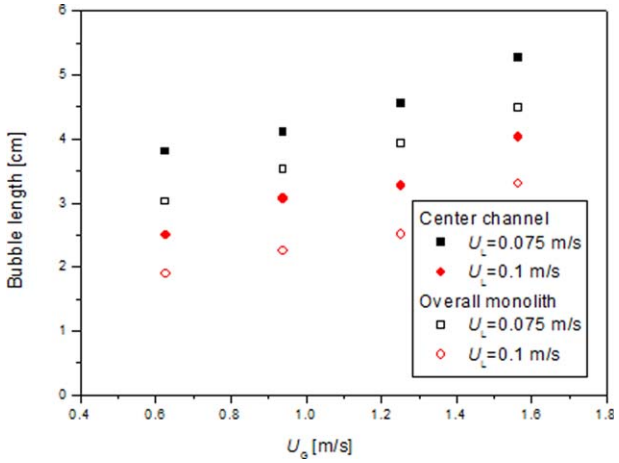

Figure 12. Bubble length of both center channel and overall monolith with varying gas and liquid superficial velocities.

[Color figure can be viewed in the online issue, which is available at wileyonlinelibrary.com.]

typically reflected in the resulting outputs shown in Figure 4, where most parts of the time series are occupied by the peaks or corresponding gas slugs with lengths of at least 5 times greater than the channel dimension. Here, the referred churn flow is different from the Taylor flow in that there exist regularly alternative gas and liquid slugs with comparable lengths in the latter flow, whereas in the churn flow,

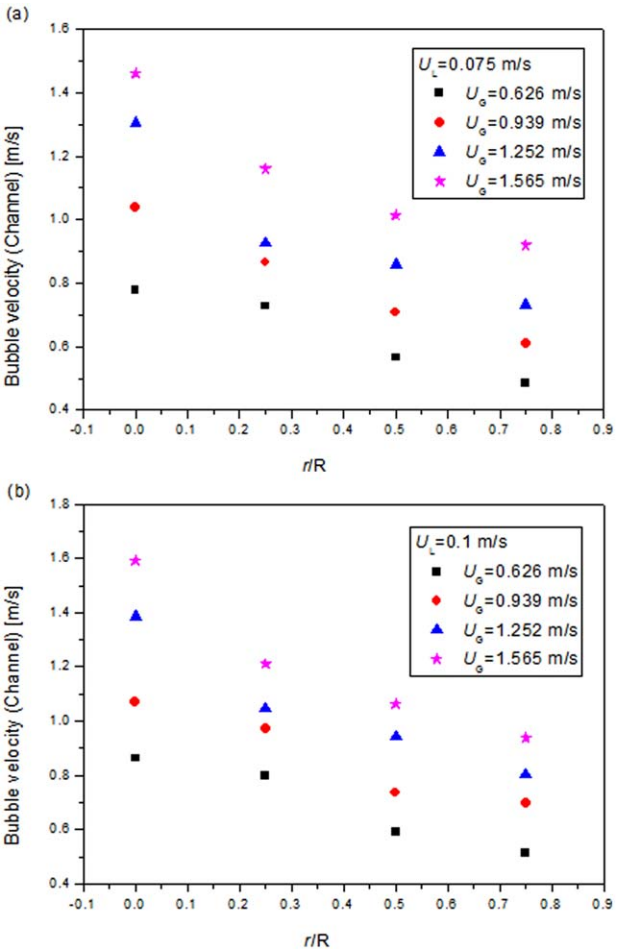

Figure 11. Radial distribution of bubble velocity. (a) U_L = 0.075 m/s and (b) U_L = 0.1 m/s.

[Color figure can be viewed in the online issue, which is available at wileyonlinelibrary.com.]

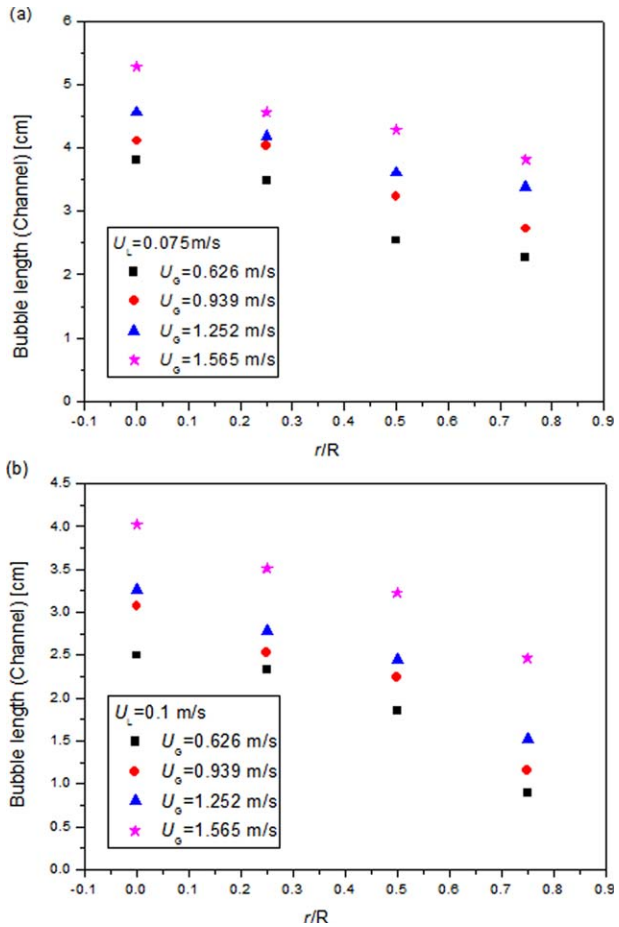

Figure 13. Radial distribution of bubble length. (a) U_L = 0.075 m/s and (b) U_L = 0.1 m/s.

[Color figure can be viewed in the online issue, which is available at wileyonlinelibrary.com.]

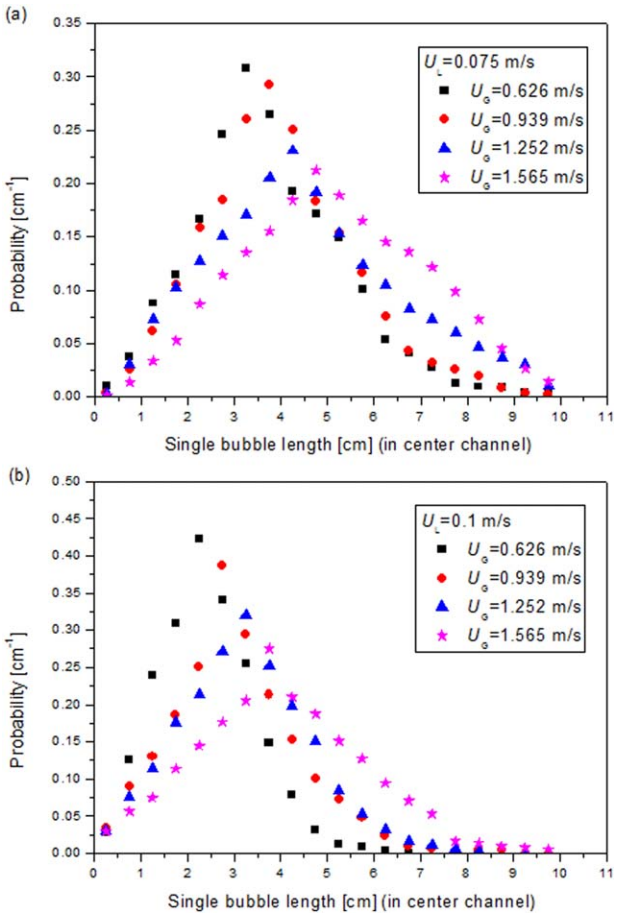

Figure 14. Probability distribution of bubble length in the center channel. (a) U_L = 0.075 m/s and (b) U_L = 0.1 m/s.

[Color figure can be viewed in the online issue, which is available at wileyonlinelibrary.com.]

very long gas bubbles are separated by short liquid slugs with similar or even less lengths to the channel dimension. In these two flows, clear-phase identification can be obtained as evidenced by the clear-cut phase signals in Figure 4. These signals are roughly square wave signals, and after a 0–1 bivalued processing, the signals are used to evaluate as follows the values of bubble parameters including gas holdup, bubble velocity, bubble frequency, and bubble length.

The local gas holdup obtained by each probe Tip XY is defined as

$$\varepsilon_{G,XY} = \frac{\text{Time spent by the probe's tip in bubbles}}{\text{Total measurement time}} = \frac{T_G}{T}(X=1,2,3,4;Y=1,2,3,4) \quad (1)$$

The gas holdup of a channel represents the average value of four local gas holdups at different axial positions in channel X.

$$<\varepsilon_{G,Y}>_X = \frac{1}{4}\sum_{Y=1}^{4}\varepsilon_{G,XY}\ (X=1,2,3,4). \quad (2)$$

The gas holdup of the overall monolith is the average value of the four selected channel holdups at different radial positions.

$$\varepsilon_G = \frac{1}{4}\sum_{X=1}^{4}<\varepsilon_{G,Y}>_X \quad (3)$$

The local bubble frequency obtained by each probe Tip XY is defined as

$$f_{b,XY} = \frac{\text{Total bubble number hitting the probe's tip}}{\text{Total measurement time}} = \frac{N_b}{T}(X=1,2,3,4;Y=1,2,3,4) \quad (4)$$

The local bubble velocity is calculated from the known axial distance between two adjacent probes, say 10 mm for $Y = 1$, 2 and $Y = 3$, 4. Single bubble velocity was calculated from the lag time between the two signals, Δt_i and the distance between the two probes, L = 10 mm, expressed by $V_{bi} = L/\Delta t_i$; see Figure 5.

The average bubble velocity is the average of the local bubble velocities

$$V_{b,XY} = \frac{1}{N_b}\sum_{i=1}^{N_b}V_{bi}\left(X=1,2,3,4;\ Y=1,2,3,4\right) \quad (5)$$

By multiplying the obtained bubble velocity $V_{b,XY}$ by the time spent by the probe's tip in each bubble T_{bi}, the single bubble length, $L_{bi} = V_{b,XY}*T_{bi}$ can be estimated.

The average of single bubble length is the average of the local bubble lengths

$$L_{b,XY} = \frac{1}{N_b}\sum_{i=1}^{N_b}L_{bi}\left(X=1,2,3,4;\ Y=1,2,3,4\right) \quad (6)$$

The calculation of the average of these parameters (bubble frequency, bubble velocity, and bubble length) in a channel and in the bed follows Eqs. (2) and (3), respectively.

Results and Discussion

As mentioned earlier, the optical fiber probes has been used for the first time inside the channels of monolithic bed to investigate and quantify key hydrodynamic parameters such as bubble and liquid slugs velocities, gas holdup, bubble and liquid slugs lengths, bubble frequency, and so forth, which are needed for integrating kinetics and hydrodynamic in performance prediction of reactor scale model,[24] and for validating CFD. In this section, the obtained results are discussed.

Gas holdup

Figure 6 shows the gas holdup of the center channel and gas holdup of the overall monolith as a function of gas velocity at two liquid velocities. Both the channel and the overall gas holdups increase with an increase in gas superficial velocity, U_G and a decrease of liquid superficial velocity, U_L. Figures 7a and b show the radial distribution of the channel gas holdup with varied gas and liquid superficial velocities. In all cases, the distribution shows a parabolic like profile with the lower end near the wall. This suggests that a great amount of liquid stays in the near wall region and accordingly reduces the amount of gas entering the channels close to the monolith walls. It was visually observed that a thick gas-liquid layer was formed just on top of the bed with more liquid being spread to the column wall region. This maldistribution of gas and liquid is due to the type of liquid distributor (nozzle) used in this study and the range of the gas and liquid velocities used. It also indicates at such range of gas and liquid

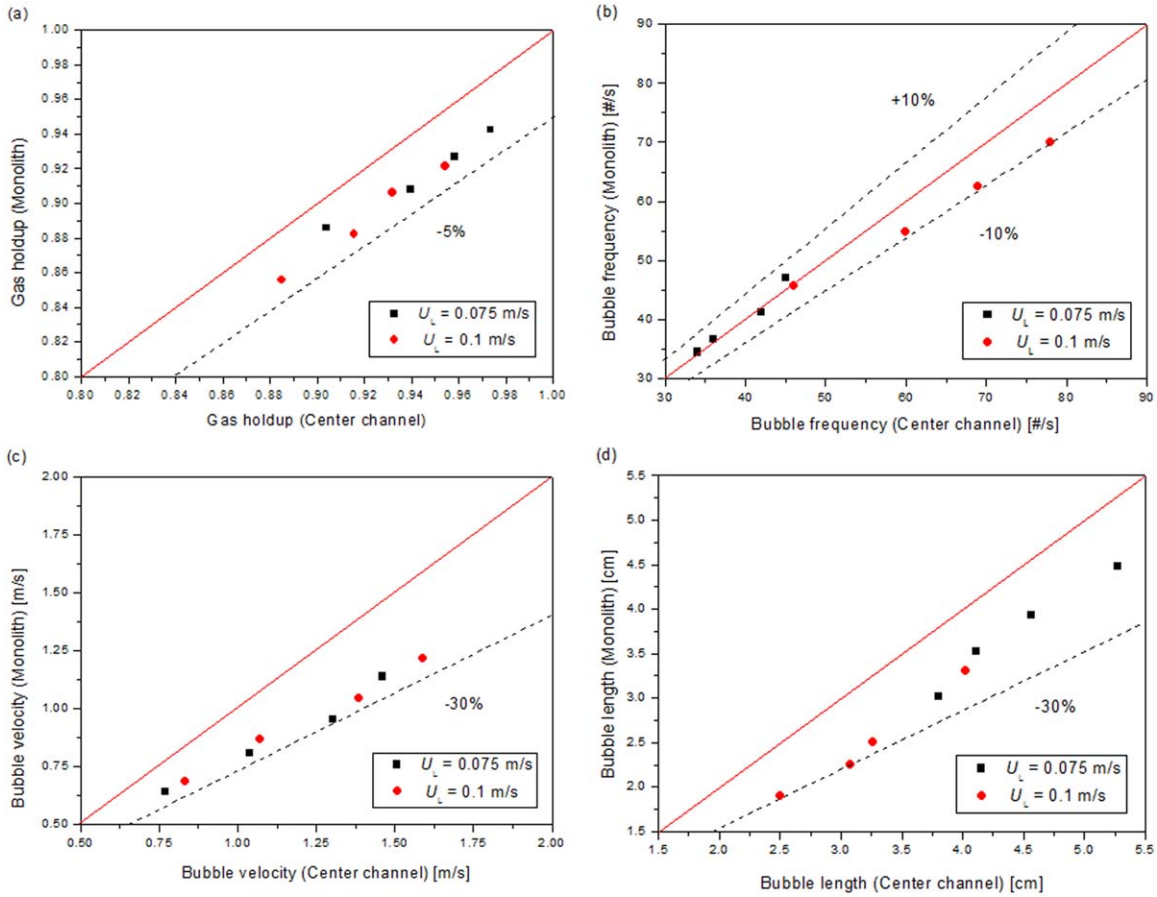

Figure 15. Comparison between the central and the bed values of: (a) gas holdup, (b) bubble frequency, (c) bubble velocity, and (d) bubble length.

[Color figure can be viewed in the online issue, which is available at wileyonlinelibrary.com.]

velocities along with the type of distributor used, uniform distribution across the core section of the bed was not obtained. Such condition necessitates the measurements of gas and liquid velocities and holdups in the channels to properly integrating kinetics and hydrodynamics for proper performance prediction of monolithic beds.

Bubble frequency

Figure 8 shows the bubble frequency of the center channel and the overall monolith bed. For both the bubble frequency increases with the increase of both gas and liquid superficial velocities. Figure 9 displays the radial distribution of the channel bubble frequency with varied gas and liquid superficial velocities. In all cases, the distribution shows a U-shaped profile along the radial direction. The competitive entrance of the gas and continuous liquid into the channels is a complicated phenomenon depending on the liquid distributor type and the local flow structure in the compartment above the monolithic bed. The bubble frequency measures the probability for bubble to enter a channel. Therefore, the U-shaped distribution of frequency implies that the layer of liquid and gas formed on the top of the bed by the nozzle distributor is nonuniform across the entrance section.

Bubble velocity

Figure 10 shows the bubble velocity for both the center channel and the overall monolith bed. The average bubble velocity of both the channel and the overall monolith bed increases with the increase of gas and liquid superficial velocities. Figure 11 displays the radial distribution of channel bubble velocity with varied gas and liquid superficial velocities. It is seen that in the wall region, bubble velocity is small because the relatively stagnant liquid phase caused by the wall and the distributor effects decrease the bubble velocity. Also the bubble velocities in the channels between the bed center and the wall are smaller than these at the center channel. This also due to the effect of how the gas and liquid are distributed at the top of the bed due to the effect of liquid distributor and the formation of nonuniform layer of liquid and gas at the top of the bed as mentioned earlier.

Bubble length

Figure 12 shows the bubble length of both the center channel and the overall monolith bed. The bubble lengths of both the channel and the overall monolith bed increase with an increase of gas superficial velocity and a decrease of liquid superficial velocity. Figure 13 displays the radial distribution of channel bubble length with varied gas and liquid superficial velocities. It is seen that the bubble length decreases toward the wall region. Figure 14 shows the probability distribution of bubble length in the center channel. In all cases, the distribution shows an inverse V-shaped profile, with the peak values corresponding to bubble lengths of about 2.0–3.0 cm. The probability distributions become

wider and the maximum probability bubble length gradually increases with the increase of gas superficial velocity at each liquid superficial velocity. The width of the probability distributions of bubble length become narrow when liquid superficial velocity increases and the maximum probability of bubble length gets higher with increasing the liquid superficial velocity.

Implications of the present results

The possibility of scale-up of gas-liquid flows from a single capillary channel to a monolith bed is an important issue for the industrial application of monolith reactors. From the discussion in the previous section, we see that the gas-liquid flows in different channels of the monolith bed are essentially not identical. To quantify the degree of such nonuniformity and evaluate the consequence of this to the scale-up of monolith reactors, the bubble parameters of the center channel are compared with the ones of overall monolith bed as shown in Figure 15. It is seen that for gas holdup (Figure 15a), bubble frequency (Figure 15b), bubble velocity (Figure 15c), and bubble length (Figure 15d), the deviations are within -5%, $\pm 10\%$, -30%, and -30%, respectively. This suggests that the flow in a single channel can not be directly translated to that on a monolithic bed scale at the studied conditions particularly with the type and operation conditions of the distributor used. These findings are due to the type of distributor used, the range of the gas and liquid flow rates used and the formed flow structure at the top of the bed. The finding is consistent with the previous finding reported by Roy,[24] where he concluded that for a distributor type, there is a range of gas and liquid flow rates where good distribution of gas and liquid would be obtained. Therefore, the reported data and the needed measurement techniques are necessary to integrate the monolith bed hydrodynamics and kinetics in a reactor scale model to properly predict the monolithic bed performance.

Concluding Remarks

The optical fiber probe has been for the first time applied to investigate the bubble dynamics and gas-phase distribution at high gas/liquid ratios in a cold flow model of monolith bed of a 0.048 m diameter and 400 cpsi. Local bubble parameters including gas holdup, bubble frequency, bubble velocity, and bubble length in individual channels were measured using 16 inserted single-point optical fiber probes mounted inside the bed. It is demonstrated that the optical fiber probe method is efficient and convenient for measuring local bubble dynamics parameters inside channels of the monolith beds. Within the range of high gas/liquid ratios under which experiments were conducted, churn flow regime occurred. In this regime, the radial distribution of gas holdup, bubble frequency, bubble velocity, and bubble length is nonuniform in nature. The radial profiles of gas holdup and bubble frequency present parabolic look and U-shape, respectively. The radial profiles of bubble velocity and bubble length both descend from center to wall region. At both the channel and the whole bed scales, bubble velocity and bubble frequency increase with the increase of both gas and liquid superficial velocities, however, gas holdup and bubble length increase with an increase in gas superficial velocity and a decrease of liquid superficial velocity. Furthermore, the probability distribution of bubble length in the center channel shows an inverse V-shaped profile, with the peak values corresponding to bubble lengths of about 2.0–3.0 cm. The probability distributions become wider and the maximum probability bubble length gradually increases with the increase of gas superficial velocity at each liquid superficial velocity. The width of the probability distributions of bubble length become narrow when liquid superficial velocity increases and the maximum probability of bubble length gets higher with increasing the liquid superficial velocity.

Acknowledgments

The financial supports provided by the State-funded Postgraduates' Overseas Study Program of China Scholarship Council (CSC) and the Coconstructing Project of both Beijing Government and the Universities in Beijing.

Literature Cited

1. Boger T, Zieverink MMP, Kreutzer MT, Kapteijn F, Moulijn J, Addiego WP. Monolithic catalysts as an alternative to slurry systems: hydrogenation of edible Oil. *Ind Eng Chem Res*. 2004;43:2337–2344.
2. Edvinsson R, Irandoust S. Hydrodesulfurization of dibenzothiophene in a monolithic catalyst reactor. *Ind Eng Chem Res*. 1993;32:391–395.
3. Klinghoffer AA, Cerro RL, Abraham MA. Influence of flow properties on the performance of the monolith froth reactor for catalytic wet oxidation of acetic acid. *Ind Eng Chem Res*. 1998;37:1203–1210.
4. Edvinsson RK, Cybulski A. A comparison between the monolithic reactor and trickle bed reactor for liquid phase hydrogenations. *Catal Today*. 1995;24:173–179.
5. Nijhuis TA, Kreutzer MT, Roumijn ACJ, Kapteijn F, Moulijn J. Monolithic catalysts as efficient three phase reactors. *Chem Eng Sci*. 2001;56:823–829.
6. Roy S, Heibel AK, Liu W, Boger T. Design of monolithic catalysts for multi-phase reactions. *Chem Eng Sci*. 2004;59:957–966.
7. Bercic G, Pintar A. The role of gas bubbles and liquid slug lengths on mass transport in the Taylor flow through capillaries. *Chem Eng Sci*. 1997;52:3709–3719.
8. Kreutzer MT, Du P, Heiszwolf JJ, Kapteijn F, Moulijn JA. Mass transfer characteristics of three-phase monolith reactors. *Chem Eng Sci*. 2001;56:6015–6023.
9. Irandoust S, Andersson B. Mass-transfer and liquid-phase reactions in a segmented two-phase flow monolithic catalyst reactor. *Chem Eng Sci*. 1988;43:1983–1988.
10. Bercic G. Influence of operating conditions on the observed reaction rate in the single channel monolith reactor. *Catal Today*. 2001;69:147–152.
11. Liu H, Vandu CO, Krishna R. Hydrodynamics of Taylor flow in vertical capillary: flow regimes, bubble velocity, liquid slug length, and pressure drop. *Ind Eng Chem Res*. 2005;44:4884–4897.
12. Qian D, Lawal A. Numerical study on gas and liquid slugs for Taylor flow in a T-junction microchannel. *Chem Eng Sci*. 2006;61:7609–7625.
13. Zhou Y, Zhang QY, Liu H, Lei ZG. Measurements and characterization of bubble dynamics in capillary two-phase flows by micro double-tip conductivity probe. *Flow Meas Instrum*. 2012;24:36–42.
14. Vandu CO, Liu H, Krishna R. Mass transfer from Taylor bubbles rising in single capillaries. *Chem Eng Sci*. 2005;60:6430–6437.
15. Roy S, Al-Dahhan M, Flow distribution characteristics of a gas-liquid monolith reactor. *Catal Today*. 2005;105:396–400.
16. Bauer T, Roy S, Lange R, Al-Dahhan M. Liquid saturation and gas-liquid distribution in multiphase monolithic reactors. *Chem Eng Sci*. 2005;60:3101–3106.
17. Behl M, Roy S. Experimental investigation of gas-liquid distribution in monolith reactors. *Chem Eng Sci*. 2008;62:7463–7470.
18. Gladden LF, Lim MHM, Mantle MD, Sederman AJ, Stitt EH. MRI visualisation of two-phase flow in structured supports and trickle-bed reactors. *Catal Today*. 2003;79–80:203–210.
19. Sederman AJ, Heras JJ, Mantle MD, Gladden LF. MRI strategies for characterising two-phase flow in parallel channel ceramic monoliths. *Catal Today*. 2007;128:3–12.

20. Mantle MD, Sederman AJ, Gladden LF, Raymahasay S, Winterbottom JM, Stitt EH. Dynamic MRI visualization of two-phase flow in a ceramic monolith. *AIChE J*. 2002;48:909–912.
21. Satterfield CN, Ozel F. Some characteristics of two-phase flow in monolithic catalyst structures. *Ind Eng Chem Fundam*. 1977;16: 61–67.
22. Mewes D, Loser T, Millies M. Modelling of two-phase flow in packings and monoliths. *Chem Eng Sci*. 1999;54:4729–4747.
23. Xu M, Huang H, Zhan XP, Liu H, Ji SF, Li CY. Pressure drop and liquid saturation in multiphase monolithic reactor with different distributors. *Catal Today*. 2009;147S:S132–S137.
24. Roy S. *Phase Distribution of Performance Studies of Gas-Liquid Monolith Reactors*. PhD Thesis. St Louis, MO: Washington University in St Louis, 2006.
25. Zhou Y, Al-Dahhan M, Dudukovic M, Liu H. Effect of distributor design on gas-liquid distribution in monolithic bed at high gas/liquid ratios. *Chin J Chem Eng*. 2012;20(4):693–700.
26. Liu W, Roy S, Fu X. Gas-liquid catalytic hydrogenation reaction in small catalyst channel. *AIChE J*. 2005;51:2285–2297.
27. Roy S, Al-Dahhan MH, Dudukovic MP, Skourlis TB, Dautzenberg FM. Countercurrent flow distribution in structured packing via computed tomography. *Chem Eng Process*. 2005;44:59–69.
28. Al-Dahhan MH, Kemoun A, Cartolano AR. Phase distribution in an upflow monolith reactor using computed tomography. *AIChE J*. 2006;52:745–753.
29. Heibel AK, Vergeldt FJ, As H, Kapteijn F, Moulijn J, Boger T. Gas and liquid distribution in the monolith film flow reactor. *AIChE J*. 2003;49:3007–3017.
30. Xue J, Al-Dahhan M, Dudukovic MP, Mudde RF. Four-point optical probe for measurement of bubble dynamics: validation of the technique. *Flow Meas Instrum*. 2008;19:293–300.
31. Xue J, Al-Dahhan M, Dudukovic MP, Mudde RF. Bubble velocity, size, and interfacial area measurements in a bubble column by four-point optical probe. *AIChE J*. 2008;54:350–363.
32. Wu C, Suddard K, Al-Dahhan MH. Bubble dynamics investigation in a slurry bubble column. *AIChE J*. 2008;54:1203–1212.

Manuscript received Sept. 6, 2012, and revision received Jun. 30, 2013.